Published in final edited form as:
Biomaterials. 2010 July ; 31(20): 5397–5407. doi:10.1016/j.biomaterials.2010.03.036.

Reducing Non-Specific Binding and Uptake of Nanoparticles and Improving Cell Targeting with an Antifouling PEO-*b*-PγMPS Copolymer Coating

Hongwei Chen[a,b], **Julie Yeh**[a,b], **Liya Wang**[a,b], **Xinying Wu**[a,c], **Zehong Cao**[d,e], **Y. Andrew Wang**[f], **Minming Zhang**[c], **Lily Yang**[d,e], and **Hui Mao**[a,b,e,*]

[a]Department of Radiology, Emory University School of Medicine, Atlanta, Georgia 30322, USA

[b]Emory Center for Systems Imaging, Emory University School of Medicine, Atlanta, Georgia 30329, USA

[c]Department of Radiology, Zhejiang University School of Medicine, Hangzhou, Zhejiang, China

[d]Department of Surgery, Emory University School of Medicine, Atlanta, Georgia 30322, USA

[e]Emory Winship Cancer Institute, Emory University, Atlanta, Georgia 30322, USA

[f]Ocean NanoTech, LLC, 2143 Worth Lane, Springdale, Arkansas 72764

Abstract

One of the major limitations impeding the sensitivity and specificity of biomarker targeted nanoparticles is non-specific binding by biomolecules and uptake by the reticuloendothelial system (RES). We report the development of an antibiofouling polysiloxane containing amphiphilic diblock copolymer, poly(ethylene oxide)-*block*-poly(γ-methacryloxypropyltrimethoxysilane) (PEO-*b*-PγMPS), for coating and functionalizing high quality hydrophobic nanocrystals such as iron oxide nanoparticles and quantum dots. These PEO-*b*-PγMPS coated nanocrystals were colloidally stable in biological medium and showed low non-specific binding by macromolecules after incubation with 100% fetal bovine serum. Both in vitro experiments with macrophages and in vivo biodistribution studies in mice revealed that PEO-*b*-PγMPS copolymer coated nanocrystals have an antibiofouling effect that reduces non-specific cell and RES uptake. Surface functionalization with amine groups was accomplished through co-crosslinking the polysiloxane coating layer and (3-Aminopropyl) trimethoxysilane in aqueous solution. Tumor integrin $\alpha_v\beta_3$ targeting peptide cyclo-RGD ligands were conjugated on the nanoparticles through a heterobifunctional linker. The resulting integrin $\alpha_v\beta_3$ targeting nanoparticle conjugates showed improved cancer cell targeting with a stronger affinity to U87MG glioma cells, which have a high expression of $\alpha_v\beta_3$ integrins, but minimal binding to MCF-7 (low expression of $\alpha_v\beta_3$ integrins).

Correspondence should be addressed to: Hui Mao, PhD, Department of Radiology, Center for Systems Imaging, Emory University School of Medicine, 1364 Clifton Road, Atlanta, GA 30322. Phone: (404) 712-0357; Fax: (404) 712-5948; hmao@emory.edu.

Keywords

Nanoparticles; Copolymer; Antifouling; Non-specific binding; Reticuloendothelial system; Cancer targeting

1. Introduction

Rapid advances in nanomedicine have led to an increasing number of nanomaterials and nanotechnologies for in vitro and in vivo biomedical applications in the areas of cancer diagnostics and therapeutics [1,2]. Nanoparticles, especially quantum dots (QDs) and metal oxide nanoparticles in the “mesoscopic” size range of 5-100 nm in diameter, often exhibit super chemical and physical properties that are not possessed by their bulk or molecular counterparts [3,4]. Many nanotechnologies and nanodevices, such as cell detection, cell separation, imaging and delivery of therapeutic agents, are developed based on the concept of targeting disease specific biomarkers or cells and have shown great potential for impacting current clinical practices [2]. Most nanoparticles developed for biomedical applications require specifically designed polymer coatings that provide a core-shell structure to stabilize nanoparticles uniformly dispersed in physiological medium while providing surface functionalities for the conjugation of biomarker targeting ligands or carrying imaging or therapeutic agents such as drugs and radioactive chelates [5-8].

Several challenges for developing functionalized nanoparticles for in vitro and in vivo biomedical applications, such as cancer targeted molecular imaging and delivery of therapeutic agents, include: 1) developing chemistries for surface functionalizations that allow for robust conjugations of payload molecules; 2) improving the stability of nanoparticles, particularly nanoparticles made in hydrophobic medium, and/or nanoparticle conjugates in blood and organs where many proteins and macromolecules may bind to nanoparticles, causing nanoparticles to aggregate and precipitate; 3) reducing non-specific absorption of biomacromolecules since they attract immune system cells and increase non-specific uptake of circulating nanoparticles by macrophages and organs in the reticular-endothelial system (RES), such as the liver and the spleen, which lead nanoparticles to be removed from circulation before reaching their tumor targets, resulting in a substantial reduction in targeting efficiency in nanoparticle-based diagnostics and therapeutics [9,10].

Solving all these problems through a single coating material platform remains challenging. For functionalized nanoparticles, coating polymers usually contain reactive functional groups, such as –COOH and $–NH_2$, which are ready for the conjugation of biomarker targeting ligands or other agents [11]. However, highly charged surfaces promote the binding of biomolecules to these nanoparticles through ionic interactions, causing particles to aggregate in biological environments [12]. Nanoparticles with high surface charges typically exhibit strong non-specific binding to various cells and tissues that is undesirable in many in vitro and in vivo applications, such as QDs based immunohistochemistry (HIC) or “nanotyping” and receptor targeted molecular imaging [13,14]. To reduce non-specific binding, a common approach is the introduction of multiple poly (ethylene glycol) (PEG) or poly(ethylene oxide) (PEO) molecules with an optimal molecular weight onto the nanoparticle surface [15,16]. PEG or PEO is known to stabilize nanoparticles in aqueous medium through both a steric effect and antibiofouling property. PEG based amphiphilic copolymer containing functional groups have been widely used to coat hydrophobic nanocrystals for biomedical applications [5,7,11,17]. However, non-specific binding in PEG coated nanomaterials remains high for some biomarker targeted applications requiring high specificity and sensitivity [18,19]. Furthermore, PEG coatings in the previous systems have

been achieved through non-covalent interactions, and there is a potential concern about the stability of these coatings in physiological medium [20-22].

Here we report our newly developed polysiloxane containing diblock copolymer: poly(ethylene oxide)-*block*-poly(γ-methacryloxypropyl trimethoxysilane) (PEO-*b*-PγMPS) for coating nanocrystals. The stability of composite nanoparticles in biological medium was tested. Non-specific binding and cell uptake and biodistribution of PEO-*b*-PγMPS copolymer coated nanoparticles were also investigated. Furthermore, we functionalized these composite nanoparticles and subsequently conjugated with the tumor integrin $\alpha_v\beta_3$ targeting tri-peptide RGD ligand. Tumor targeting ability of RGD conjugated IONPs was tested using U87MG glioma cells with high expressions of $\alpha_v\beta_3$.

2. Materials and methods

2.1. Materials

γ-Methacryl oxypropyltrimethoxysilane (γMPS, 98%, Aldrich) was purified by distillation under reduced pressure. 2,2-Azobis(isobutyronitrile) (AIBN, 98%, Aldrich) used as an initiator was purified by recrystallization in ethanol. Sulfosuccinimidyl-*4*-(*N*-maleimidomethyl) cyclohexane-*1*-carboxylate (Sulfo-SMCC, Pierce Biotechnology), fluorescein isothiocyanate (FITC, Pierce Biotechnology), and Cyclo (Arg-Gly-Asp-*D*-Phe-Cys) (RGD-SH, Peptides International, Inc) were used as received. Carbon disulfide (99.9%), magnesium turnings (>99.5%), 2-chloro-2-phenylacetyl chloride (CPAC, 90%), poly(ethylene oxide) monomethyl ether (PEO) (M_n = 5000 g/mol, M_w/M_n = 1.10), anhydrous dioxane (99.8%), anhydrous tetrahydrofuran (THF, 99.8%), (3-Aminopropyl) trimethoxysilane (APTMS) and all other chemicals were purchased from Aldrich.

2.2. Preparation of IONPs and QDs

Hydrophobic iron oxide nanocrystals were prepared by heating iron oxide powder and oleic acid in octadecene at 315 °C [23]. CdSe/ZnS nanocystals with emission peaks at 608 nm were prepared using the typical successive ionic layer adsorption and reaction or solution atomic layer epitaxy techniques [24]. Water soluble nanocrystals coated with amphiphilic block copolymers [25] as a control were prepared using the approach for QDs developed by Gao et al [17]. Amphiphilic block copolymer coated IONPs were further conjugated with PEG2000 to produce PEG blocked nanoparticles. Other control samples include commercial QDs (Qdot@605ITK, Invitrogen) and IONPs (FeRex, Biopal). The physical properties of the various surface-modified nanoparticles we used in this study are summarized in Table 1.

2.3. Synthesis of PEO-*b*-PγMPS diblock copolymer

PEO-*b*-PγMPS diblock copolymer was synthesized by the reversible addition fragmentation chain transfer (RAFT) polymerization which we previously reported [18]. Briefly, the polymerization was performed in a schlenk flask with γMPS (1.2 mL, 5 mmol), PEO macro-chain transfer agent (PEO-CTA) (0.69 g, 0.12 mmol), and AIBN (7.1 mg, 0.04 mmol) along with anhydrous 1,4-dioxane (2 mL). The purified copolymer confirmed by both NMR and GPC was dissolved in anhydrous THF to form a solution with a concentration of 50 mg/mL.

2.4. Stabilizing IONPs and QDs with the PEO-*b*-PγMPS diblock copolymer

The method for transferring hydrophobic nanocrystals into water is the same as previously published [18]. Briefly, the nanocrystals were mixed with the newly synthesized copolymer in anhydrous THF. After being aged for 4 days, the mixture was added dropwise into water with gentle magnetic stirring. THF in the solution was removed by dialysis using deionized water. For IONPs, the solution was then purified by using a magnetic separator (Frantz laboratory). This wash-resuspend step was repeated three times. The final iron concentration

was determined by spectrophotometry [26]. For QDs, the solution was first centrifuged at 6,000 rpm for 10 min followed by 14,000 rpm for 10 min to remove the small amount of large aggregates. The collected supernatant was then isolated by ultracentrifugation at 100,000 rpm for 20 min. The solid was re-suspended and ultracentrifugation was repeated. The final concentration of QDs was determined by the molar extinction coefficient [27]. The average hydrodynamic diameter and size distribution of composite nanoparticles were measured using a dynamic light scattering (DLS) instrument (Malvern Zeta Sizer Nano S-90) equipped with a 22 mW He-Ne laser operating at $\lambda = 632.8$ nm. The core sizes of co-polymer coated nanocrystals and thickness of polymer layers were viewed and measured by transmission electron microscopy (TEM) (Hitachi H-7500 instrument (75 kV)). A drop of diluted solution was put on the grid and air-dried. Absorption spectra were obtained with a scanning spectrophotometer (Shimadzu UV-2401PC) with a slit width of 1.0 nm. Photoluminescence spectra were acquired using a spectrofluorometer (SPEX FluoroMax-2) with a 450 nm excitation and a 5.0 nm width slit for the excitation and emission monochromators.

2.5. Cell culture and preparation

The A549 lung cancer cell line, U87MG brain cancer cell line, MCF-7 breast cancer cell line and RAW 264.7 macrophage cell line were maintained as an adherent culture and grown as a monolayer in a humidified incubator (95% air; 5% CO_2) at 37 °C in a Petri dish containing medium supplemented with pen-strep and 10% heat-inactivated fetal bovine serum (FBS). The RAW 264.7 macrophage and A549 lung cancer cell lines were kept in RPMI, while the U87MG and MCF-7 cancer cells were incubated in DMEM further supplemented with antibiotic-antimycotic and non-essential amino acids solutions.

2.6. In vitro cell cytotoxicity analysis

The A549 cell line was used to measure the cytotoxicity of PEO-*b*-PγMPS block copolymer and amphiphilic block copolymer coated nanocrystals in vitro. 10^5 cells were plated in each well of a 96-well plate 24 h before washing with PBS (pH 7.4) and adding nanoparticles at selected concentrations. After 12 h of incubation, the solutions were removed and cells were washed three times with PBS. Cell viability was then estimated using the MTT conversion test. Briefly, 100 μL of the MTT solution was added to each well. After incubation for 4 h, each well was treated with 100 μL of DMSO with pipetting for 5 min. Absorption at 570 nm was measured on a plate reader. Readings from the four wells were averaged, and 100% viability was determined for untreated cells.

2.7. Uptake of nanoparticles by macrophage cells in vitro

We selected macrophages (RAW 264.7) for testing non-specific cell uptake of the polymer coated nanoparticles. Cells were seeded into an 8-well chamber slide and left overnight. After exposure to IONPs at concentrations of 0.1 mg/mL and 0.025 mg/mL iron per well in Hanks solution for 1 h at 37 °C, cells were washed with PBS, and then fixed with 0.5 mL of 4% paraformalin (PFA) for 20 min. Prussian blue staining was used to determine the presence of iron in the cells. Each well of the chamber slide was filled with 0.5 mL of 5% potassium ferrocyanide (II) trihydrate and 5% HCl solution and incubated for 15 min. After being washed three times with distilled water, cells were counterstained with nuclear fast red solution for 5 min. After consecutive dehydrations with 70% and 100% EtOH and two rinses in xylene, the slide was mounted. The result of Prussian blue staining was assessed by a light microscope. After being treated with QDs at particle concentrations of 10 nM and 20 nM per well in Hanks solution for 2 h at 37 °C, cells were washed with PBS, then fixed with 0.5 mL of 4% PFA for 20 min. The image was visualized via fluorescence microscopy.

2.8. Biodistribution of nanoparticles with different polymer coatings in mice

For in vivo biodistribution of IONPs with different polymer coatings, all animal experiments were carried out with mice. 6-8 week-old BALB/c mice (N = 5/group) were injected intravenously via the tail vein with different polymer coated IONPs (10 mg/Kg Fe of body weight) in 100 μL PBS solution. At 24 h post-injection, the mice were sacrificed. The liver, spleen, kidney and brain were excised from each animal and washed with PBS solution. Tissues from mice not receiving IONPs were used as the control. The iron content of mice organs were determined by inductively coupled plasma-optical emission spectrometry (ICP-OES). For analysis, the tissue samples were frozen and then placed in a Labconco FreeZone 4.5 Freeze Dry system for 24 h until all moisture had been removed. All tissue samples were then weighted on a certified analytical balance (Mettler AE200) and placed into individual porcelain crucibles that were washed with 10% HCl acid and sterilized at 700 °C for 4 h. The samples were then placed into a digital muffle furnace set (Fisher Scientific) at 500 °C for 4 h to ash the tissue matrix. Once ashed and cooled, samples were dissolved in 1 mL of tissue buffer solution containing 20 ppm Molybdenum certified standard as an internal sample standard and ran on the Thermo Jarrell-Ash Enviro 36 ICP-OES, which was set up with a 20 element sweep. Fe content in each organ was subtracted by the corresponding averaged value for its control.

For in vivo biodistribution of QDs, mice were treated with 1.5 nmol of QDs with different polymer coatings, which were injected intravenously into the tail vein. At 24 h post-injection, the mice were sacrificed. The liver, spleen, kidney, lung, heart, muscle, and brain were excised and washed with PBS solution. Mice organs were imaged using the Olympus OV100 small animal imaging system (Olympus Corp, Japan) containing an MT-10 light source (Olympus Biosystems, Germany). Fluorescent images were collected with an exposure time of 100 ms using RFP filter sets with an excitation filter of BP545 and an emission filter of BA570-625.

2.9. Surface functionalization of PEO-*b*-PγMPS coated nanoparticles

2 mL of 1.8 mg/mL water soluble IONPs solution was added with 80 μL APTMS solution (80 μL APTMS in 800 μL DMSO). The reaction was carried out at room temperature with gentle stirring for two days. The resultant solution was purified through a PD-10 column (GE, Healthcare). To confirm whether the amine group can be used for conjugating bioactive ligands, we tested the conjugation with fluorescein isothiocyanate (FITC). 1 mL of 0.8 mg/mL functionalized IONPs with 0.1 M sodium carbonate was mixed slowly with 2 mg FITC in 200 μL anhydrous DMSO with gentle stirring for 2 h at room temperature in the dark. Afterwards, the reaction solution was dialyzed against 0.1 M sodium carbonate solution with changes of fresh buffer at 0.5 h, 1.5 h, and 2.5 h. Then the solution was run through a PD-10 column and produced two clearly separated bands corresponding to the faster moving band with FITC conjugated IONPs and the slower moving band with free FITC. The first band was collected. To get rid of any free FITC, we filtered the solution using a 100K Pall nanosep® filter (Pall Corp.) at 5000 rpm for 10 min twice until there was no obvious change in the fluorescent intensity.

2.10. Conjugating RGD ligands to functionalized IONPs

For RGD-coupling, IONPs functionalized with amine groups were dissolved with sodium carbonate to form a 0.1 M solution with a pH of 9. This solution was then combined with the Sulfo-SMCC solution at a 1000:1 linker/particle molar ratio. The reaction proceeded for 1 h in the dark at room temperature, and the resulting product was purified with a PD-10 column. A small amount of 0.1 M sodium carbonate solution was added to the collected solution to adjust the pH to 7.5. Subsequently, RGD-SH was added slowly in about 100

folds excess amount. This reaction was carried out for 1 h in the dark at room temperature. The free RGD-SH was removed by a PD-10 column.

2.11. Prussian blue staining of iron in cells treated with integrin targeting RGD-IONPs

Approximately 10^5 U87MG cells with high $\alpha_v\beta_3$ expression or MCF-7 cells with low $\alpha_v\beta_3$ expression were seeded in each cell culture chamber on the day before incubation. Cells were fixed with PFA for 20 min right before the addition of IONPs. Afterwards, 100 nM RGD-IONPs or IONPs in binding buffer [9] (20 mM Tris, 150 mM NaCl, 2 mM $CaCl_2$, 1 mM $MnCl_2$, 1 mM $MgCl_2$, 0.1% (wt/vol) bovine serum albumin; pH 7.4) were added into the culture chamber, and the incubation was performed at room temperature for 2 h with gentle shaking. The particles were then removed, and the cells were washed three times with PBS buffer. Subsequently, cells were stained with Prussian blue and nuclear fast red and then mounted to be visualized.

2.12. MRI of cells treated with integrin targeting RGD-IONPs

For making cell samples for MRI experiments, RGD-IONP bound cells were washed with PBS and then scraped from the flasks. Collected cells were re-suspended in 1 ml of 2% agarose gel at 50 °C in a glass tube before the mixture cooled to room temperature and solidified for MRI scans. All MRI experiments were performed on a 3 Tesla MR scanner (Magnetom Tim Trio, Siemens Medical Solutions, Erlangen, Germany) using a standard head coil with samples placed in the iso-center of the magnet. T_2 weighted fast spin echo sequence was used for scanning the cell samples treated with RGD-IONPs.

To measure the transverse relaxation time T_2 as well as to generate a T_2 relaxometry map of each sample, a multi-echo spin echo sequence was used with *TR* of 2000 ms and 20 *TE*s starting at 10 ms with increments of 10 ms. The value of the T_2 relaxation time was calculated from the measured average signal intensity values *I* at different *TE*s using a non-linear exponential curve fitting based on Equation [1]:

$$I = K_2 e^{-TE/T_2} \quad [1]$$

where K_2 is also a catch-all gain constant for each sample.

3. Results and discussions

3.1. Stability of PEO-*b*-PγMPS coated nanoparticles in aqueous medium

The diblock copolymer PEO-*b*-PγMPS was successfully developed by RAFT polymerization using a PEO macro chain transfer agent (CTA). The chemical structures of this CTA as well as its copolymer were reported in our previous paper [18]. The copolymer PEO-*b*-PγMPS was selected as a coating material for hydrophobic nanocrystals based on several considerations. First of all, we selected the PEO as one block because PEO is commonly used to improve biocompatibility and systemic circulation [15]. Secondly, selecting PγMPS as the other block offers a reactive trimethoxysilane group in this segment, which can act as an “anchor” on the surface of IONPs through the ligand exchange so that we can make hydrophobic nanoparticles water soluble [28]. Furthermore, this diblock copolymer is amphiphilic and can self-assemble to form a polysiloxane coating layer on hydrophobic nanoparticles when it collapses on the surface of nanoparticles during the process of being transferred to water [29]. As a result, the cross-linked polysiloxane layer along with the hydrophilic PEO offer the double protections to stabilize the nanoparticle from aggregation. Finally, the cross-linked polysiloxane layer with low surface charges may minimize non-specific uptake of the composite nanoparticles.

Figure 1a shows the hydrodynamic size distribution of the composite IONPs in water. The composite IONPs had an averaged diameter of 24 nm measured by DLS. With the 13 nm IONP core, IONPs appeared to be mono-dispersed with the coating polymer protecting against aggregation in water. The thickness of the polymer shell was estimated at about 5-6 nm, indicating a single diblock copolymer layer covering around the IONPs. The overall size of this polysiloxane coated nanoparticles is favorable for biomedical applications in vivo since previous reports suggested that IONPs with hydrodynamic diameter smaller than 30 nm have a longer mean blood circulation time and better tissue penetration [4, 30]. The TEM image of such composite IONPs dried from aqueous solution and shown in the insert of Figure 1a further reveal the mono-distributed IONPs with an intact polymer shell. A monolayer coating without particle aggregations indicates that the copolymer works well for coating oleic acid stabilized IONPs. Although the contrast of the polymer is low in TEM images, a thin polymer layer around the uniformly sized nanoparticles is still visible. The thickness of the polysiloxane coating layer measured with TEM is around 3-5 nm, which is slightly lower than the hydrodynamic size estimated from DLS measurement.

Similar to stabilization of IONPs in water, this copolymer can also be used to transfer hydrophobic QDs into water. The DLS result in Figure 1b shows that composite QD nanoparticles had an averaged hydrodynamic size of 11 nm. The TEM image (insert in Figure 1b) shows a good dispersion of QDs and measurement of the 5 nm core size supported the result measured by DLS. The UV-vis and fluorescence measurements shown in Figure 1c reveal that the unique optical properties of QDs are not greatly affected by this copolymer coating when transferring QDs from the organic phase to the aqueous solution. The absorption peak of QDs in water does not shift compared to that in chloroform. However, the fluorescent intensity of these QDs in water decreased when compared to parental powder in chloroform [20, 31]. Nevertheless, the QDs were quite stable once they were coated by the PEO-*b*-PγMPS copolymer in water as shown in Figure 1d. A picture of the solutions of both IONPs and QDs coated by PEO-*b*-PγMPS copolymer is shown in Figure 1e. The IONP solution can be stored at 4 °C for at least 6 months without any change in hydrodynamic size as monitored by DLS. For QDs, there was no obvious change in the fluorescent intensity after storing at 4 °C for 1 month; however, there was a 3-nm blue shift, suggesting that QDs may be slowly eroded in water.

3.2. Stability of nanoparticles in biological medium

We tested the stability of the PEO-*b*-PγMPS copolymer coated nanoparticles in medium similar to physiological conditions. PEO-*b*-PγMPS copolymer coated IONPs were stable in PBS buffer as well as in 1 M concentrated salt solution and did not exhibit any change in hydrodynamic size (See Figure S1a). Both of these are typical conditions used in biological applications. Figure S1b also reveals that copolymer coated IONPs can tolerate a wide range of pH conditions from pH 2-12. Such properties may be attributed to the almost neutral coating layer composed of PEG and crosslinkable polysiloxane.

To verify the stability and antibiofouling of PEO-*b*-PγMPS copolymer IONPs under physiological conditions that contain various bioactive macromolecules, we monitored the hydrodynamic size change of IONPs using DLS after incubating IONPs with PBS and fetal bovine serum (FBS) without dilution [12,32]. These results are shown in Table 2. After mixing PEO-*b*-PγMPS copolymer coated IONPs with FBS, there was no increase in the hydrodynamic size for up to 8 hours based on the intensity weighted hydrodynamic size as measured by DLS, which is more sensitive to large particles. The slight decrease in size compared to that in PBS may be attributed to the scattering intensity contributed by proteins in the medium. In comparison, the hydrodynamic size increased by 33 nm for the amphiphilic block copolymer coated IONPs and 28 nm for dextran coated IONPs from FeRex within 5 minutes after mixing with FBS (see detailed information in Figure S2). We

attribute these hydrodynamic size changes to the absorption of proteins in the medium through electrostatic interactions. The results indicate that PEO-*b*-PγMPS coating polymers offer considerable antibiofouling properties.

3.3. Cytotoxicity of the PEO-*b*-PγMPS polymer coating

The MTT assay using the A549 cell line was performed to analyze the possible toxicity of the PEO-*b*-PγMPS coated IONPs and QDs. Our results indicate that both IONPs and QDs showed no toxicity even at relatively high concentrations (See Figure S3). The amount of iron at the highest concentration was 0.5 mg/mL Fe which far exceeds that of iron used in typical IONP-based MR contrast enhancing experiments in mice (1-20 mg Fe/Kg of body weight). The toxicity of QDs is a particular concern for in vivo applications because they contain toxic metal ions. Nevertheless, the cell viability results from this study showed that there was no cytotoxicity to A549 cells observed even at the 100 nM concentration, which is 100 times higher than the dosage used in reported studies [14].

3.4. Reduced non-specific uptake by macrophage cells in vitro

Since macrophages are a main component of the immune system, they were used to test the non-specific uptake of nanoparticles [33]. The uptake of PEO-*b*-PγMPS coated nanoparticles by macrophages was compared with that of conventional amphiphilic block copolymers [25] and PEG blocked IONPs as shown in Figure 2, respectively. After 1 h of incubation of each IONP sample with macrophages, Prussian blue staining was carried out to detect the presence of IONPs in the cells. We did not observe any blue stains for the cells treated with PEO-*b*-PγMPS polymer coated IONPs at two different concentrations (0.1 and 0.025 mg/mL Fe), which was comparable to the control sample in which cells were not treated with any particles (Figures 2a to 2c). For the block copolymer coated IONPs with carboxyl groups on the surface, substantial blue staining was observed around the cell membrane in both concentrations as shown in Figures 2d-2e, suggesting a strong non-specific uptake of IONPs by macrophages. The non-specific cellular binding of nanoparticles with a highly negatively charged surface is consistent with previously reported observations [19]. After blocking the carboxyl groups using PEG, non-specific uptake was reduced, but we still observed an obvious uptake of PEG coated IONPs at the higher iron concentration (0.1 mg/mL Fe) as shown in Figures 2f-2g. This maybe attributed to the incomplete blocking of carboxyl groups after PEGylation. The comparisons clearly indicate that the PEO-*b*-PγMPS coating polymer can greatly reduce non-specific uptake by macrophages likely due to its almost neutral surface.

This reduced non-specific uptake was also confirmed by optical microscopy using PEO-*b*-PγMPS polymer coated QDs and two commercialized QDs with different coatings. The non-specific binding of QDs to macrophage cells was visualized by fluorescent microscopy as shown in Figure 3. Cells incubated with PEO-*b*-PγMPS coated QDs were seen with typical background and without any bright red from QDs (Figures 3b-3c), indicating no uptake or binding of QDs by the macrophage cells even with a concentration of up to 20 nM [14]. However, for cells treated with amphiphilic block copolymer coated QDs (Figures 3d-3e) and QDs from Invitrogen (Qdot@605ITK) (Figures 3f-3g), a bright orange-red was seen due to the combination of red from the QDs and green background from the cells, indicating a large amount of non-specific uptake of QDs. The non-specific binding problem may cause a high level of background fluorescence that can reduce the contrast-to-noise ratio and limit the sensitivity and specificity of biomarker targeted detection.

3.5. Reduced non-specific uptake of PEO-*b*-PγMPS coated nanoparticles by RES in mice

The fate of nanoparticles following intravenous administration is determined by their polymer coatings. After nanoparticles are injected into the bloodstream, they usually are

rapidly bound by macromolecules such as proteins in the plasma circulation [34]. This process is known as opsonization and is critical in dictating the outcome of the injected nanoparticles. Normally, opsonization renders the particles recognizable by the body's major defense system, the RES. The macrophages of the liver and to a lesser extent the macrophages of the spleen and circulation, therefore, play a critical role in the removal of opsonized particles [35]. However, for many applications of nanoparticles in vivo, such as tumor targeted drug delivery and imaging, RES "trapping" of nanoparticles leads to substantial reductions in targeting efficiency and potential toxicity to the normal organs. As a result, the application of nanoparticles in vivo would require surface modifications that would evade the RES to improve targeting efficiency. Figure 4 shows the biodistribution of IONPs with different coatings in major organs in mice. The results reveal that the polysiloxane-containing polymer coated IONPs had the lowest uptake by both liver and spleen. This RES evading capability is likely attributed to the high stability and antibiofouling property of PEO-*b*-PγMPS coated nanoparticles in physiological conditions. The higher uptake of amphiphilic block copolymer coated IONPs was observed in both the liver and spleen and is likely due to high surface charges (zeta potential ~ −35 mV) and ease of non-specific binding with plasma proteins [36]. Compared to commercially available dextran coated IONPs from Biopal (FeRex), PEO-*b*-PγMPS coated IONPs exhibited 29% and 49% lower iron content in the liver and spleen, respectively.

Reduced in vivo non-specific uptake of PEO-*b*-PγMPS copolymer coated nanoparticles by RES was also observed in optical imaging after intravenous injection of PEO-*b*-PγMPS copolymer coated QDs. Figure 5 shows the fluorescent images of mice organs. Similar to control mice without any QD injections, the organs from mice injected with PEO-*b*-PγMPS copolymer coated QDs did not show any emission, but an expected red fluorescence from QDs in the liver of mice receiving amphiphilic block copolymer coated QDs and Qdot@605ITK from Invitrogen was noted. The observation of liver uptake of QDs is consistent with previous observations [25,37]. The results from the RES uptake study with QDs confirmed again that PEO-*b*-PγMPS coated nanoparticles show reduced RES uptake.

3.6. Functionalization of PEO-*b*-PγMPS coated IONPs

For tumor-specific delivery of imaging probes and therapeutic agents, PEO-*b*-PγMPS copolymer coating was functionalized using APTMS, which has been widely used to functionalize silicon coated nanoparticles [38,39]. We modified the polysiloxane coating with amine groups through a co-crosslink between silanol and APTMS in aqueous solution. Figure 6 shows the scheme of amine group functionalized PEO-*b*-PγMPS copolymer coated IONPs and bioconjugation with the small peptide RGD. Since the copolymer forms a thin polysiloxane coating layer (3-5 nm) and hydrophilic PEO outer layer, the functionalization using APTMS can be successfully carried out in aqueous medium without any IONP aggregation. However, the functionalization is very sensitive to the molecular weight of the polymer, the molar ratio between APTMS and IONPs and the reaction time. The zeta potential measurement was used to confirm the functionalization with amine groups. After amine modification, there was no obvious change in the hydrodynamic size, but there was a remarkable increase in zeta potential from -9.1 ± 0.4 to $+14.2 \pm 0.9$ mV, which indicated the presence of amine groups on the surface of the IONPs [40]. The negatively charged surface before amine functionalization is attributed to the partially hydrolyzed silanol groups [41]. To further confirm the existence of amine groups, we conjugated FITC, which is widely used to attach a fluorescent label to proteins via the amine group. After conjugation, the zeta potential was decreased to -33.2 ± 4.7 mV due to the replacement of amine groups with FITC, which contains negatively charged carboxyl groups. The absorption peak at 495 nm as shown in Fig. 7 and the emission peak at 520 nm as shown in the insert clearly reveal the conjugation of FITC to the coating polymer. Based on the absorption intensity and the

standard curve of FITC in DMSO, it was estimated that the average number of FITC on each particle is about 1×10^4 which is very close to the theoretical value. Since we post-functionalized the surface, we can adjust the number of functional groups by varying the molar ratio of APTMS/nanoparticles.

Tumor-targeted nanoparticles as potential carrier vectors of therapeutic agents are believed to be the next promising platform for nanobiotechnology. Differences in the expression of cellular receptors between normal and tumor cells represent a great opportunity for targeting nanoparticles to cancer cells. For engineering tumor targeted nanoparticles, different ligands targeting the related receptors that are highly expressed in tumor cells are usually conjugated to the surface coating polymer of nanoparticles [25]. Small peptide RGD has been widely used in conjugations with nanoparticles to target $\alpha_v\beta_3$ highly expressed cells [42]. To test the improved tumor targeting with PEO-*b*-PγMPS copolymer coated IONPs, we conjugated RGD-SH to the amine groups of IONPs through a two-step protocol using a heterobifunctional linker, SulfoSMCC [43]. Resulting RGD-IONP conjugates had a negative charge of -8.0 ± 0.5 mV, almost the same as before the surface functionalization and conjugation. We then used $\alpha_v\beta_3$ positive U87MG human glioblastoma cells and $\alpha_v\beta_3$ negative MCF-7 human breast cancer cells to test the binding affinity of RGD-IONPs [9]. Cells were treated with either IONPs or RGD-IONPs. As seen in Figure 8a, Prussian blue staining for iron showed that there was no non-specific cellular binding of PEO-*b*-PγMPS copolymer coated IONPs to U87MG cells. In contrast, incubation of $\alpha_v\beta_3$ highly over expressed U87MG cells with $\alpha_v\beta_3$ targeting RGD-IONPs led to substantial positive Prussian blue staining, indicating the binding of RGD-IONPs to the U87MG cell membrane (Figure 8b). However, Prussian blue staining was negative in MCF-7 cells treated with RGD-IONPs, suggesting no binding of RGD-IONPs to $\alpha_v\beta_3$ negative MCF-7 cells (Figure 8c). IONPs are known for their strong effect of shortening the transverse T_2 relaxation time which generate *T*2 weighted contrast, typically signal drops, in magnetic resonance imaging (MRI). T_2 weighted fast spin echo MRI of U87MG cells treated with RGD-IONPs showed significant signal drops and reduction of transverse T_2 relaxation time, indicating the cells are labeled with targeting IONPs (Figure 8d).

The contrast between cancer targeted RGD-IONPs and non-targeting IONPs is important to the development of cancer targeting nanoparticle imaging agents and drug delivery. The results of high contrast between targeted IONPs and non-targeted IONPs with PEO-*b*-PγMPS copolymer coatings suggest that functionalized PEO-*b*-PγMPS copolymer coated IONPs can greatly improve cancer cell targeting with reduced non-specific cellular uptake.

4. Conclusions

Amphiphilic diblock copolymer PEO-*b*-PγMPS was developed to transform and stabilize hydrophobic IONPs and QDs in water. A combined PEO and crosslinkable polysiloxane coating layer resulted in copolymer coated nanocrystals with nearly neutral surface charge and significant reductions in both non-specific binding of nanoparticles by macromolecules and uptake of nanoparticles by the RES, which was confirmed by both in vitro cell binding and uptaking experiments and in vivo biodistribution studies. This reduction in non-specific uptake may increase circulation time and decrease organ toxicity. Furthermore, we demonstrated that these antibiofouling composite nanoparticles can be conjugated with tumor targeting ligands, such as integrin $\alpha_v\beta_3$ targeting small peptide RGD, for cancer targeted imaging and drug delivery.

Supplementary Material

Refer to Web version on PubMed Central for supplementary material.

Acknowledgments

This work in part is supported by the Emory-Georgia Tech Nanotechnology Center for Personalized and Predictive Oncology of NIH NCI Center of Cancer Nanotechnology Excellence (CCNE, U54 CA119338-01 to HM and LY), Emory Molecular Translational Imaging Center of NIH in vivo Cellular and Molecular Imaging Center grant (ICMIC, P50CA128301-01A10003 to HM and LY), and a research grant from EmTech Bio, Inc.

References

1. Kim J, Piao Y, Hyeon T. Multifunctional nanostructured materials for multimodal imaging, and simultaneous imaging and therapy. Chem Soc Rev. 2009; 38:372–90. [PubMed: 19169455]
2. Kim J, Lee JE, Lee SH, Yu JH, Lee JH, Park TG, et al. Designed fabrication of a multifunctional polymer nanomedical platform for simultaneous cancer-targeted imaging and magnetically guided drug delivery. Adv Mater. 2008; 20:478–83.
3. Michalet X, Pinaud FF, Bentolila LA, Tsay JM, Doose S, Li JJ, et al. Quantum dots for live cells, in vivo imaging, and diagnostics. Science. 2005; 307:538–44. [PubMed: 15681376]
4. Jun YW, Lee JH, Cheon J. Chemical design of nanoparticle probes for high-performance magnetic resonance imaging. Angew Chem Int Ed. 2008; 47:5122–35.
5. Smith AM, Duan HW, Rhyner MN, Ruan G, Nie SM. A systematic examination of surface coatings on the optical and chemical properties of semiconductor quantum dots. Phys Chem Chem Phys. 2006; 8:3895–03. [PubMed: 19817050]
6. Lees EE, Nguyen TL, Clayton AHA, Mulvaney P. The preparation of colloidally stable, water-soluble, biocompatible, semiconductor nanocrystals with a small hydrodynamic diameter. Acs Nano. 2009; 3:1121–28. [PubMed: 19388661]
7. Yu WW, Chang E, Falkner JC, Zhang JY, Al-Somali AM, Sayes CM, et al. Forming biocompatible and nonaggregated nanocrystals in water using amphiphilic polymers. J Am Chem Soc. 2007; 129:2871–79. [PubMed: 17309256]
8. Jain TK, Foy SP, Erokwu B, Dimitrijevic S, Flask CA, Labhasetwar V. Magnetic resonance imaging of multifunctional pluronic stabilized iron-oxide nanoparticles in tumor-bearing mice. Biomaterials. 2009; 30:6748–56. [PubMed: 19765817]
9. Cai WB, Chen XY. Preparation of peptide-conjugated quantum dots for tumor vasculature-targeted imaging. Nat Protoc. 2008; 3:89–6. [PubMed: 18193025]
10. Doshi N, Mitragotri S. Designer biomaterials for nanomedicine. Adv Funct Mater. 2009; 19:3843–54.
11. Duan HW, Kuang M, Wang XX, Wang YA, Mao H, Nie SM. Reexamining the effects of particle size and surface chemistry on the magnetic properties of iron oxide nanocrystals: new insights into spin disorder and proton relaxivity. J Phys Chem C. 2008; 112:8127–31.
12. Boyer C, Priyanto P, Davis TP, Pissuwan D, Bulmus V, Kavallaris M, et al. Anti-fouling magnetic nanoparticles for siRNA delivery. J Mater Chem. 2010; 20:255–65.
13. Pathak S, Choi SK, Arnheim N, Thompson ME. Hydroxylated quantum dots as luminescent probes for in situ hybridization. J Am Chem Soc. 2001; 123:4103–04. [PubMed: 11457171]
14. Duan HW, Nie SM. Cell-penetrating quantum dots based on multivalent and endosome-disrupting surface coatings. J Am Chem Soc. 2007; 129:3333–38. [PubMed: 17319667]
15. van Vlerken LE, Vyas TK, Amiji MM. Poly(ethylene glycol)-modified nanocarriers for tumor-targeted and intracellular delivery. Pharm Res. 2007; 24:1405–14. [PubMed: 17393074]
16. Sheng Y, Liu CS, Yuan Y, Tao XY, Yang F, Shan XQ, et al. Long-circulating polymeric nanoparticles bearing a combinatorial coating of PEG and water-soluble chitosan. Biomaterials. 2009; 30:2340–48. [PubMed: 19150737]
17. Gao XH, Cui YY, Levenson RM, Chung LWK, Nie SM. In vivo cancer targeting and imaging with semiconductor quantum dots. Nat Biotechnol. 2004; 22:969–76. [PubMed: 15258594]
18. Chen HW, Wu XY, Duan HW, Wang YA, Wang LY, Zhang MM, et al. Biocompatible polysiloxane-containing diblock copolymer PEO-b-PγMPS for coating magnetic nanoparticles. Acs Appl Mater Inter. 2009; 1:2134–40.

19. Kairdolf BA, Mancini MC, Smith AM, Nie SM. Minimizing non-specific cellular binding of quantum dots with hydroxyl-derivatizied surface coatings. Anal Chem. 2008; 80:3029–34. [PubMed: 18324840]
20. Uyeda HT, Medintz IL, Jaiswal JK, Simon SM, Mattoussi H. Synthesis of compact multidentate ligands to prepare stable hydrophilic quantum dot fluorophores. J Am Chem Soc. 2005; 127:3870–78. [PubMed: 15771523]
21. Choi HS, Ipe BI, Misra P, Lee JH, Bawendi MG, Frangioni JV. Tissue- and organ-selective biodistribution of NIR fluorescent quantum dots. Nano Lett. 2009; 9:2354–59. [PubMed: 19422261]
22. Amstad E, Gillich T, Bilecka I, Textor M, Reimhult E. Ultrastable iron oxide nanoparticle colloidal suspensions using dispersants with catechol-derived anchor groups. Nano Lett. 2009; 9:4042–48. [PubMed: 19835370]
23. Yu WW, Falkner JC, Yavuz CT, Colvin VL. Synthesis of monodisperse iron oxide nanocrystals by thermal decomposition of iron carboxylate salts. Chem Commun. 2004:2306–07.
24. Li JJ, Wang YA, Guo WZ, Keay JC, Mishima TD, Johnson MB, et al. Large-scale synthesis of nearly monodisperse CdSe/CdS core/shell nanocrystals using air-stable reagents via successive ion layer adsorption and reaction. J Am Chem Soc. 2003; 125:12567–75. [PubMed: 14531702]
25. Yang LL, Mao H, Wang YA, Cao ZH, Peng XH, Wang XX, et al. Single chain epidermal growth factor receptor antibody conjugated nanoparticles for in vivo tumor targeting and imaging. Small. 2009; 5:235–43. [PubMed: 19089838]
26. Nitin N, LaConte LEW, Zurkiya O, Hu X, Bao G. Functionalization and peptide-based delivery of magnetic nanoparticles as an intracellular MRI contrast agent. J Biol Inorg Chem. 2004; 9:706–12. [PubMed: 15232722]
27. Yu WW, Qu LH, Guo WZ, Peng XG. Experimental determination of the extinction coefficient of CdTe, CdSe, and CdS nanocrystals. Chem Mater. 2003; 15:2854–60.
28. Jana NR, Earhart C, Ying JY. Synthesis of water-soluble and functionalized nanoparticles by silica coating. Chem Mater. 2007; 19:5074–82.
29. Du JZ, Chen YM, Zhang YH, Han CC, Fischer K, Schmidt M. Organic/inorganic hybrid vesicles based on a reactive block copolymer. J Am Chem Soc. 2003; 125:14710–11. [PubMed: 14640638]
30. Neuberger T, Schopf B, Hofmann H, Hofmann M, von Rechenberg B. Superparamagnetic nanoparticles for biomedical applications: possibilities and limitations of a new drug delivery system. J Magn Magn Mater. 2005; 293:483–96.
31. Nikolic MS, Krack M, Aleksandrovic V, Kornowski A, Forster S, Weller H. Tailor-made ligands for biocompatible nanoparticles. Angew Chem Int Ed. 2006; 45:6577–80.
32. Yang W, Zhang L, Wang SL, White AD, Jiang SY. Functionalizable and ultra stable nanoparticles coated with zwitterionic poly(carboxybetaine) in undiluted blood serum. Biomaterials. 2009; 30:5617–21. [PubMed: 19595457]
33. Lee H, Lee E, Kim DK, Jang NK, Jeong YY, Jon S. Antibiofouling polymer-coated superparamagnetic iron oxide nanoparticles as potential magnetic resonance contrast agents for in vivo cancer imaging. J Am Chem Soc. 2006; 128:7383–89. [PubMed: 16734494]
34. Berry CC, Curtis ASG. Functionalisation of magnetic nanoparticles for applications in biomedicine. J Phys D Appl Phys. 2003; 36:R198–06.
35. Araujo L, Lobenberg R, Kreuter J. Influence of the surfactant concentration on the body distribution of nanoparticles. J Drug Target. 1999; 6:373–85. [PubMed: 10342385]
36. Chouly C, Pouliquen D, Lucet I, Jeune JJ, Jallet P. Development of superparamagnetic nanoparticles for MRI: effect of particle size, charge and surface nature on biodistribution. J Microencapsul. 1996; 13:245–55. [PubMed: 8860681]
37. Choi HS, Liu W, Misra P, Tanaka E, Zimmer JP, Ipe BI, et al. Renal clearance of quantum dots. Nat Biotechnol. 2007; 25:1165–70. [PubMed: 17891134]
38. Kang K, Choi J, Nam JH, Lee SC, Kim KJ, Lee SW, et al. Preparation and characterization of chemically functionalized silica-coated magnetic nanoparticles as a DNA separator. J Phys Chem B. 2009; 113:536–43. [PubMed: 19099431]

39. Niu DC, Li YS, Qiao XL, Li L, Zhao WR, Chen HR, et al. A facile approach to fabricate functionalized superparamagnetic copolymer-silica nanocomposite spheres. Chem Commun. 2008:4463–65.

40. Lee H, Yu MK, Park S, Moon S, Min JJ, Jeong YY, et al. Thermally cross-linked superparamagnetic iron oxide nanoparticles: synthesis and application as a dual imaging probe for cancer in vivo. J Am Chem Soc. 2007; 129:12739–45. [PubMed: 17892287]

41. Bagwe RP, Hilliard LR, Tan WH. Surface modification of silica nanoparticles to reduce aggregation and non-specific binding. Langmuir. 2006; 22:4357–62. [PubMed: 16618187]

42. Zhang CF, Jugold M, Woenne EC, Lammers T, Morgenstern B, Mueller MM, et al. Specific targeting of tumor angiogenesis by RGD-conjugated ultrasmall superparamagnetic iron oxide particles using a clinical 1.5-T magnetic resonance scanner. Cancer Res. 2007; 67:1555–62. [PubMed: 17308094]

43. Chen K, Xie J, Xu HY, Behera D, Michalski MH, Biswal S, et al. Triblock copolymer coated iron oxide nanoparticle conjugate for tumor integrin targeting. Biomaterials. 2009; 30:6912–19. [PubMed: 19773081]

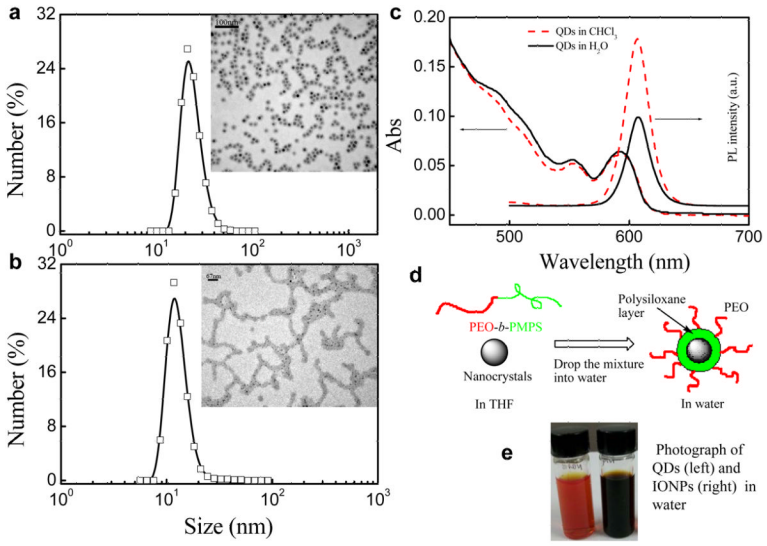

Fig. 1.

a) The hydrodynamic size distribution and TEM image (insert) of PEO-*b*-PγMPS coated IONPs, and b) QDs, c) Optical absorption and fluorescence spectra of QDs in $CHCl_3$ and PEO-*b*-PγMPS coated QDs in water, d) Scheme of PEO-*b*-PγMPS making hydrophobic nanocrystals water soluble, e) Photograph of PEO-*b*-PγMPS coated IONPs and QDs in water.

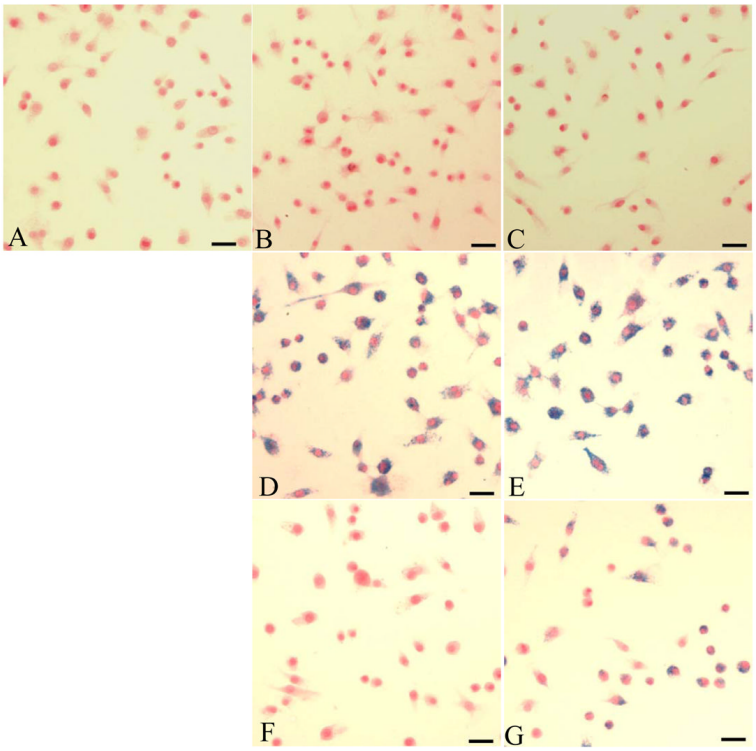

Fig. 2.

Prussian blue stained images of macrophage cells, RAW 264.7, after treatment with or without different IONP samples. a) Control: without any particles, b-c) PEO-*b*-PγMPS coating, d-e) Amphiphilic triblock copolymer coating, and f-g) PEG block. Cells in b, d, and f were incubated with IONPs with a concentration of 0.1 mg/mL Fe; cells in c, e, and g were incubated with IONPs with a concentration of 0.025 mg/mL Fe. Scale bar, 50 μm.

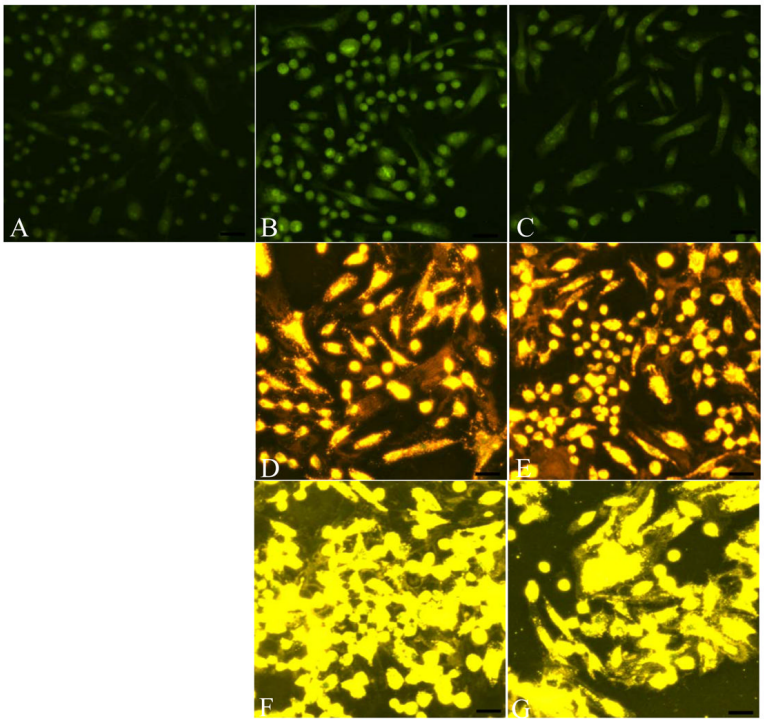

Fig. 3.

Non-specific uptake of QDs with different coatings visualized via fluorescent microscopy. a) Control: without any particles, b-c) PEO-*b*-PγMPS coating, d-e) Amphiphilic triblock copolymer coating, and f-g) Invitrogen samples (Qdot@605ITK). Cells in b, d, and f were incubated with 10 nM QDs; cells in c, e, and g were incubated with 20 nM QDs. Scale bar, 50 μm.

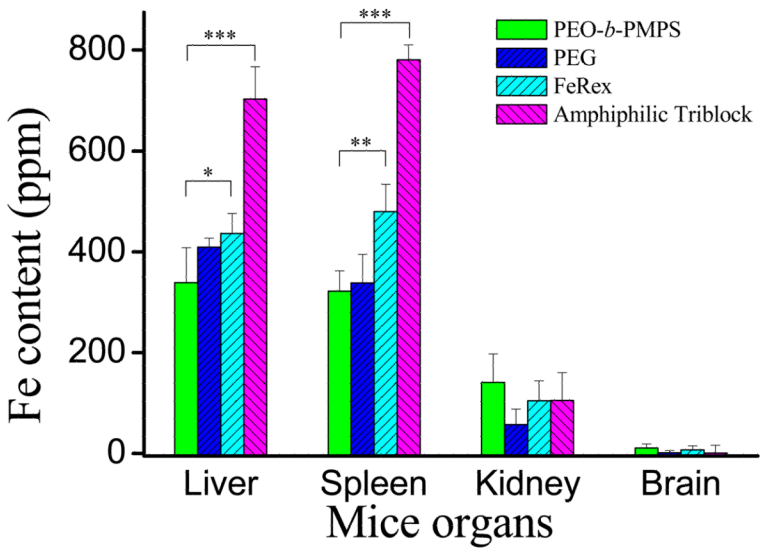

Fig. 4.

Fe content in the mouse organs as analyzed by ICP-OES. Data were obtained from the mice receiving IONPs with different coatings. Organs were collected 24 h post-injection. $N = 5$ in each group. Data are expressed as means and standard deviations. The iron content differences in the liver and spleen with different coatings are statistically significant with $*p < 0.05$, $**p < 0.01$, $***p < 0.001$.

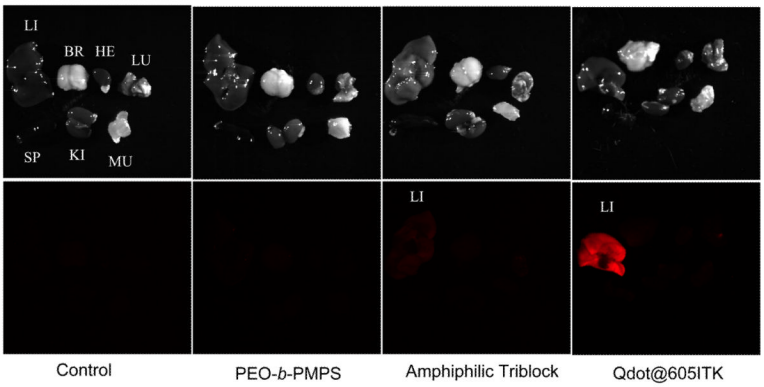

Fig. 5.

Photographic images (top) and corresponding optical fluorescence images (bottom) of mice organs with deposition of QDs coated with different coatings. Each mouse was injected with 1.5 nmol QDs through the tail. Organs were collected and imaged 24 h post-injection. Organs in each picture are: liver (LI), brain (BR), heart (HE), lung (LU); spleen (SP), kidney (KI), muscle (MU).

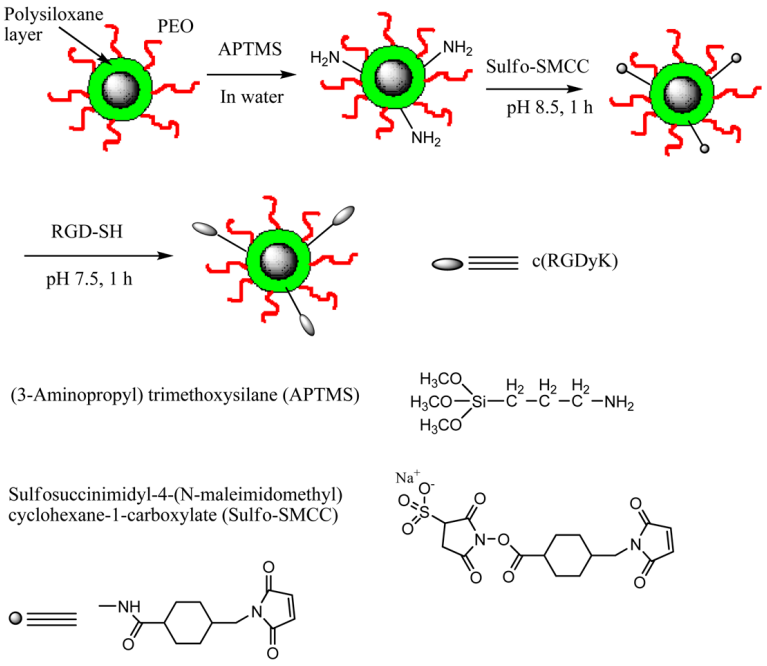

Fig. 6.

Schematic of nanoparticle with PEO-*b*-PγMPS coating and its functionalization with amine groups as well as subsequent RGD conjugation.

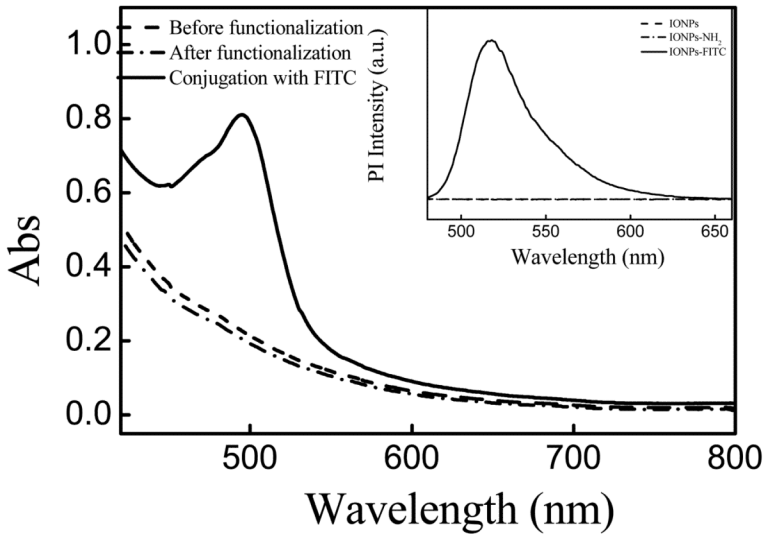

Fig. 7.

Optical absorption and fluorescent spectra (insert) of PEO-*b*-PγMPS coated IONPs, amine group functionalized IONPs, and FITC conjugated IONPs.

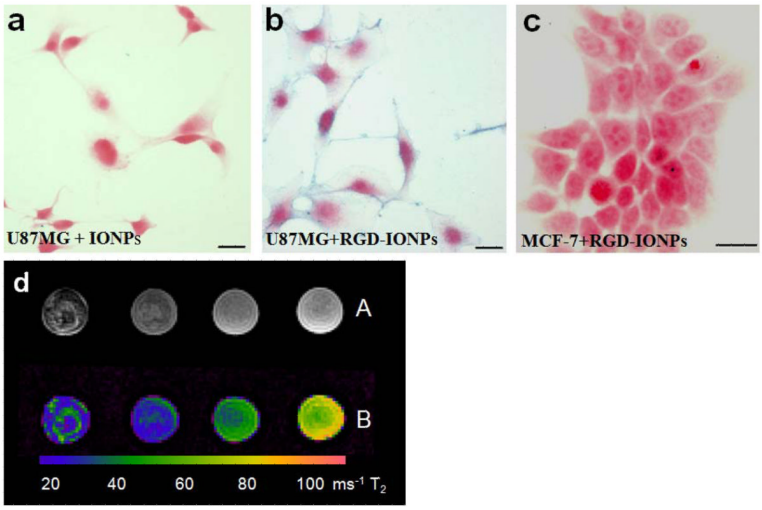

Fig. 8.

Prussian blue staining of iron after incubating IONPs (a) or RGD-IONPs (b) with U87MG cells, respectively and RGD-IONPs treated MCF-7 cells (c). Scale bar, 50 μm. (d) T_2 weighted MRI (A) of cell phantoms containing 5, 2 and 1×10^6 U87MG cells bound with tumor integrin targeted RGD-IONP conjugates (left to right) showed different levels of MRI signal drops in the T_2 weighted spin echo images and reduction of T_2 relaxation times in T_2 maps (B). The control sample (far right) contains 2×10^6 U87MG cells without IONPs.

Table 1

Sizes and zeta potentials of various surface-modified nanoparticles.

Samples	IONPs with coating from				QDs with coating from		
	PEO-*b*-PγMPS	**Amphiphilic block**	**PEG**	**FeRex Biopal**	**PEO-*b*-PγMPS**	**Amphiphilic block**	**Invitrogen, QD605ITK**
Size /nm	23.7	19.4	26.8	18.0	11.2	9.7	9.1
Zeta Potential /mV	−9.1	−35.1	−29.6	−30.7	−6.4	−23.6	−38.0

Note: hydrodynamic size was fitted by number weight and zeta potential was measured at pH 6.5. IONPs with coating from PEG refer to PEG blocked amphiphilic block.

Table 2

Hydrodynamic size of IONPs with different coatings after incubation with PBS and FBS for 8 h.

IONPs with coating from	PEO-*b*-PγMPS	Amphiphilic block copolymer	FeRex from Biopal
In PBS /nm	32.4 ± 0.5	49.6 ± 0.4	125.3 ± 0.6
In FBS /nm	30.2 ± 0.4	83.0 ± 1.3	153.7 ± 1.1

Note: hydrodynamic size was fitted by intensity weight.